International Journal of Applied Pharmaceutics

ISSN- 0975-7058 Vol 15, Special Issue 1, 2023

Original Article

ENHANCEMENT OF CURCUMIN SOLUBILITY AND DISSOLUTION BY ADSORPTION IN MESOPOROUS SBA-15

LILI FITRIANI*, HUSNUN AZIZAH, USWATUL HASANAH, ERIZAL ZAINI

Department of Pharmaceutics, Faculty of Pharmacy, Universitas Andalas, Kampus Limau Manis, Padang 25163
***Email: lilifitriani@phar.unand.ac.id**

Received: 12 Nov 2022, Revised and Accepted: 03 Jan 2023

ABSTRACT

Objective: Curcumin belongs to BCS class IV, which has low solubility, around 7.8 µg/ml and its results of low bioavailability. The study aimed to enhance solubility and dissolution rate of curcumin by adsorption in mesoporous silica SBA-15.

Methods: The synthesis of SBA-15 was done by using tetraethyl orthosilicate (TEOS) as silica precursors and Pluronic P123 (EO20PO70EO20) as template of pore-forming. Impregnation of curcumin in SBA-15 was conducted by evaporation in ethanol solution with 2:1 of curcumin: SBA-15 proportion. Curcumin-SBA-15 were characterized by Nitrogen Adsorption-Desorption Isotherm, Powder X-Ray Diffraction (PXRD), Fourier Transformed Infrared (FT-IR), Differential Scanning Calorimetry (DSC), and Scanning Electron Microscopy (SEM). The solubility test was performed by using an orbital shaker for 24 h in CO_2-free distilled water. The dissolution rate was conducted in CO_2-free distilled water using USP Type-II dissolution test apparatus.

Results: Efficiency entrapment of curcumin-SBA-15 was 59.433%. The successful adsorption of curcumin in SBA-15 was confirmed by reducing its surface area (48.165 m^2/g) and pore volume ($0.073x10^{-1}$ cm^3/g). The results of PXRD analysis showed that decreased in the intensity of the diffraction peak. In addition, the FTIR spectrum of curcumin-SBA-15 was similar to its intact component. The solubility and dissolution rate test of curcumin-SBA-15 enhanced 2.201 times and 3.214 times at 60 min compared to intact curcumin.

Conclusion: It can be concluded that the adsorption of curcumin in SBA-15 increased both the solubility and dissolution rate of curcumin.

Keywords: Curcumin, SBA-15, Solubility, Dissolution rate

DOI: https://dx.doi.org/10.22159/ijap.2023.v15s1.47515 Journal homepage: https://innovareacademics.in/journals/index.php/ijap

INTRODUCTION

Curcumin (CUR) is the most active component of Turmeric (*Curcuma longa* L.), which has several therapeutic benefits, including antioxidant, antimicrobial and anti-carcinogenic, and anti-inflammatory, one of the most difficult challenges in developing curcumin is low oral bioavailability due to its hydrophobicity. Curcumin belongs to Biopharmaceutics Classification System (BCS) class IV in which the solubility is around 7.8 µg/ml and resulting limit its efficacy [1, 2]. Several methods have been developed to improve the solubility of the compound, such as solid lipid nanoparticle, solid dispersion, colloidal drug delivery systems, microemulsion and multicomponent crystal [3, 4].

A mesoporous material have attracted a great deal of interest in the past decade because of specific features which are well-ordered pores, high surface area and high porosity. Mesoporous materials consist from silica and non-silica substance like mesoporous oxide metal with nitrate salt precursor from the metals Zn, Ni, Co, Pb, Al. However, non-silica mesoporous have a high reactivity in condensation and hydrolysis reaction from oxide metal precursor, resulting an unstable mesoporous. Thus, mesoporous silica is more commonly used than non-silica [5].

Mesoporous silica has been proven to enhance the solubility and dissolution rate of poor soluble drugs. The inclusion of carbamezapine in MCM-41 mesoporous, which has synthesized using cetyltrimethylammonium chloride (CTACl) showed that the dissolution MCM-41-CARBA reached 97% in deionised water, 90% in phosphate buffer and 83% compared to the crystalline form the drug release was only 60%, 65% and 35%, respectively [6]. In addition, ketoprofen into SBA-15 showed increasing its solubility up to 95% in acidic and basic pH [7].

In this study, SBA-15 mesoporous silica is used due to thick pore walls so will present better thermal stability than MCM-41. SBA-15 is synthesized using nonionic surfactant (normally containing triblock-copolymers) which can used as a template of pore-forming. In the acidic solution, surfactant will organize the micelles formation and coated by silica precursor tetraethyl ortho-silicate (TEOS). Mesoporous silica SBA-15 was obtained by removing surfactant with calcination method in the high temperature. Therefore, this study aims to prepare curcumin in SBA-15 mesoporous by adsorption process in order to enhance the solubility and dissolution of curcumin. The mesoporous are characterized by Nitrogen Adsorption-Desorption Isotherm, Powder X-Ray Diffraction (PXRD), Fourier Transformed Infrared (FT-IR), Differential Scanning Calorimetry (DSC), Scanning Electron Microscopy (SEM) [8, 9].

MATERIALS AND METHODS

Materials

Curcumin (Tokyo Chemical Industry, Japan), Pluronic P123 ($[HO(CH_2CH_2O)_{20}(CH_2CH(CH_3)O)_{70}(CH_2CH_2O)_{20}H]$) (Sigma Aldrich, US), TEOS (Tetraethyl Ortho-Silicate) (Sigma Aldrich, US), hydrochloric acid, ethanol, sodium chloride and deionized water.

Methods

Preparation of SBA-15

Synthesis of mesoporous silica SBA-15 was performed by molar ratio of TEOS: HCl: H2O: P123 as 1:6:166:0.02 with the addition of 6 moles of NaCl. In a typical synthesis process, Pluronic 123 and NaCl were dissolved in 2 M hydrochloric acid (HCl) and deionized water, stirred for 24 h at room temperature. Tetraethyl ortho-silicate (TEOS) was added, a clear solution was achieved after 3 h of continuous mechanical stirring of the solution then stored at 80 ^{0}C for 24 h as for hydrothermal process. The white solid product was washed and filtered with deionized repeatedly and dried at 50 °C. The removal of the surfactant template was achieved by calcination in 550 °C for 4 h to form SBA-15 [10].

Adsorption of curcumin in SBA-15

Curcumin was dissolved in ethanol (10 mg/ml) and SBA-15 was added in the weight ratios 2:1 (curcumin: SBA-15). Then, the mixture was stirred with a magnetic stirrer at a temperature of 80

°C at 300 rpm until the solvent evaporated and produced curcumin-SBA-15 powder.

Characterization of SBA-15 and curcumin in SBA-15

1. Nitrogen adsorption-desorption isotherm analysis

This measurement was conducted based on isothermal adsorption-desorption using nitrogen gas (Quantachrome novatouch LX-4, US). SBA-15 was degassed at 150 °C to obtain P/Po and BET value transformation [1/W(P/Po)]. The surface area of SBA-15 and curcumin loaded in SBA-15 was calculated using the Brunauer-Emmett-Teller (BET) method [11].

2. Differential scanning calorimetry (DSC) analysis

Differential scanning calorimeter was used to record DSC thermograms (Shimadzu DSC-60 Plus, Japan). SBA-15, curcumin-SBA-15 and curcumin were scanned progressively by increasing the temperature from 20 to 250 °C at a heating rate of 10 °C/min. Melting process produce endothermic peak in DSC thermograms when the temperature was increased [12].

3. Fourier transformed infrared (FT-IR) analysis

SBA-15, curcumin-SBA-15 and curcumin were analyzed using FT-IR (Shimadzu IRTracer-100, Japan) by placing them directly on the sampling plate of on window optics with crystal ZnSe, then held by a clamp compression micrometer controlled for ensure good contact among samples and crystals. Measurement of sample performed on the range wave number 4000-400 cm^{-1} [13].

4. Scanning electron microscopy (SEM) analysis

SEM Analysis (Hitachi FLEXSEM 100, Japan) was conducted with method by placing SBA-15, curcumin-SBA-15 and curcumin on surface sample holder that has been containing carbon type; then conducted coating layered gold so that surface sample could be detected by SEM [11].

5. Powder X-ray diffraction (PXRD) analysis

Powder X-ray diffraction (PANanalytical MPD PW3040/60 type X'Pert Pro, Netherlands) was used Cu Kα radiation (λ = 1.5406) with acceleration voltage and current 40 kV and 40 mA to determine the crystallinity of the samples and structural properties of the pure then functionalized SBA-15 with 2θ in the range 5-50° with a scan interval of 0.02°. The result of this analysis is forming of a curve among the intensity peak diffraction sample and 2θ [11].

Solubility test

Solubility test was performed for curcumin and curcumin-SBA-15 by adding an excess amount of samples in 100 ml of CO_2-free distilled water. Then, the samples were shaken with an orbital shaker at rate 100 rpm and temperature at 25 °C for 24 h. The amount of curcumin dissolved was analyzed by using a UV-Visible spectrophotometer at 426 nm. The solubility test of each sample was performed in triplicated.

Dissolution test

The dissolution of curcumin and curcumin-SBA-15 was conducted using dissolution type II (Type Paddles) at rate 100 rpm in 900 ml CO_2 free distilled water and sodium lauryl sulfate (SLS) 0.1% as the medium at 37 °C±0.5 °C. The amount of curcumin dissolved was calculated in 5, 10, 15, 30, 45, 60 min using UV-Vis spectrophotometer at 426 nm. The dissolution test was done in triplicated.

RESULTS

Nitrogen adsorption-desorption isotherm

Characterization of nitrogen adsorption-desorption isotherm of SBA-15 and curcumin-SBA-15 is shown in table 1. Isotherm curve of N_2 adsorption-desorption was presented in fig. 1 and N_2 gas adsorption occurs by physisorption that could use in porous material characterization because of the adsorption of N_2 could release back (desorption), then measured the surface area [14].

Table 1: Pores characteristic of SBA-15 and curcumin-SBA-15

Parameter	SBA-15	Curcumin-SBA-15
Surface Area (m^2/g)	343.563	48.165
Pore Volume ($x\ 10^{-1}\ cm^3/g$)	4.879	0.073
Pore Diameter (nm)	R= 2.841 or D= 5.682	R = 3.020 or D = 6.040

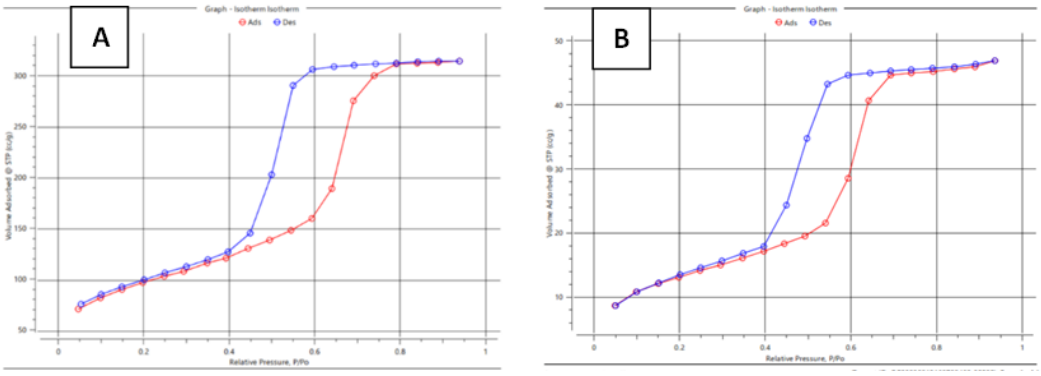

Fig. 1: Isotherm curves A) SBA-15 and B) curcumin-SBA-15

Based on isotherm curve of N_2 adsorption-desorption, the pore size of SBA-15 and curcumin-SBA-15 were 2-50 nm that indicated the size pore of mesoporous. Both of them showed type IV isotherm, which is characteristic of mesoporous materials as defined by IUPAC. Moreover, the curve isotherm shows hysteresis loops at 0.4-0.8 of relative pressure (P/P0) with sharp adsorption and desorption branches. When relative pressure is increased, the adsorption of adsorbates, molecules first adsorb onto the pore surface area as a single layer to multilayer, indicating condensation capillary of mesoporous. Then, whole surface pores already full filled and the relative pressure was decreased to show desorption as seen in the illustration of fig. 2. The hysteresis loops have a diameter of 3-6 nm, which was in accordance with the result of other study [15, 16]. Due to not all of N_2 could be released properly, hysteresis loops or gaps between curve adsorption and desorption occurred. The isotherm curve of desorption will always be on top compared to curve of adsorption, which showing that N_2 desorbed occurs at a lower pressure than the required pressure of adsorption [17].

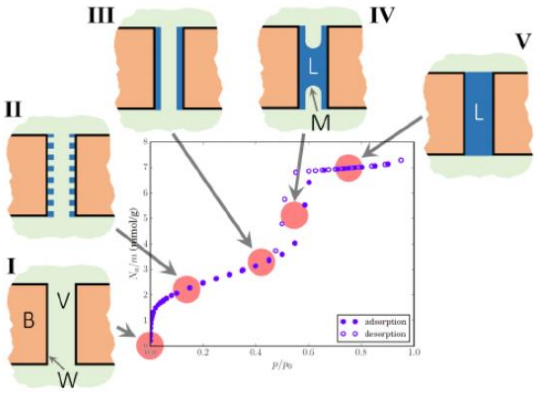

Fig. 2: Illustration scheme from adsorption-desorption nitrogen

The surface area and pore volume in SBA-15 is larger than curcumin-SBA-15. Surface area of SBA-15 was 343.563 m^2/g decreased to 48.165 m^2/g in curcumin-SBA-15. Similar to the pore volume of SBA-15 which has 4.879 x 10^{-1} cm^3/g reduced to 0.073 x 10^{-1} cm^3/g in the curcumin-SBA-15. The significant reductions in surface area of the loaded samples when compared to SBA-15 confirm the good adsorption of curcumin within the pores. The diameter of pore on SBA-15 and curcumin-SBA-15 are not different for each other that indicate the mesoporous has good stability [18, 19].

Powder X-ray diffraction (PXRD) analysis

Diffractogram pattern from PXRD analysis for curcumin, SBA-15 and curcumin-SBA-15 is shown in fig. 3 and table 2, with formation peaks at a typical 2θ for each component with intensity certain.

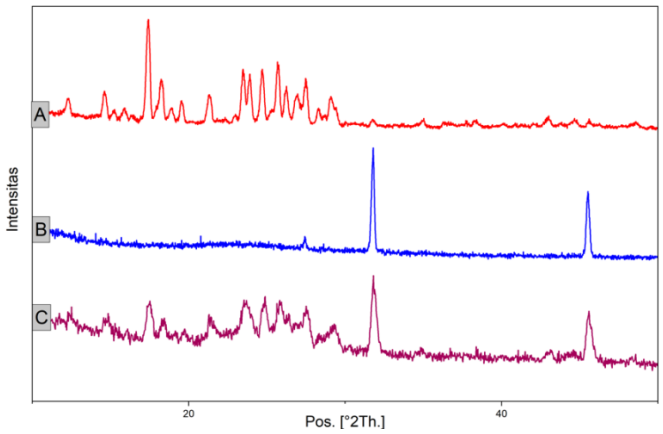

Fig. 3: Diffractogram X-Ray A) Curcumin, B) SBA-15, and C) Curcumin-SBA-15

Table 2: Intensity peak PXRD of curcumin, SBA-15 and curcumin-SBA-15

Position 2θ (°)	Intensity		
	Curcumin	SBA-15	Curcumin-SBA-15
12.30	511.968	264.682	266.050
14.61	605.682	213.988	259.851
17.42	1531.584	175.960	325.723
18.24	760.272	195.019	260.914
23.47	886.929	183.270	322.924
24.70	886.814	197.195	318.041
25.68	981.569	184.741	302.296
26.25	668.668	173.575	283.065
27.48	768.717	240.463	306.965
31.79	234.119	959.644	446.464
45.51	201.575	615.479	306.807

Curcumin is in the crystalline state form that shown from distinctive and sharp peaks intensity. Peak diffraction curcumin in position 2θ are 12.3°; 14.61°; 17.42°; 18.24°; 23.47°; 24.70°; 25.68°; 26.25° and 27.48° which also appropriate with research that has been conducted previously. Meanwhile, PXRD peak intensities of curcumin-SBA-15 was lower than SBA-15 due to pore filling of curcumin which reduced the crystallinity of curcumin in table 2. This is consistent with previously reported results by Allazawi, *et al.* showing that decreasing intensity of adsorption amoxicillin in SBA-15 [18, 20].

Fourier-transformed infrared (FT-IR) analysis

Characterization using FTIR spectrophotometer aims to identify group function on a compound based on differences movement vibration from molecules that stick together bond. Spectrum results absorption infrared on the sample of curcumin, SBA-15 and

curcumin-SBA-15 can be seen in fig. 4.

In the spectrum of SBA-15 observed that there is absorption on wave number 3399.78 cm^{-1} which shows existence group hydroxyl (-OH). The band locate at 467.54 cm^{-1} show the presence of Si-O-Si bending. Absorption Si–O–Si vibration asymmetric bending found at 1055.83 $cm^{-1}$and symmetric stretching at 800.96 cm^{-1}. According to Albayati, *et al.* who have conducted that peak 1100 $cm^{-1}$is present absorptionSi–O–Si asymmetric bending, the spectrum that appears about 800 cm^{-1} signify presence of Si–O–Si symmetric stretching and absorption of Si–O–Si bending seen 400 cm^{-1}(19). The results of the FTIR spectrum obtained in the study this has in accordance with literatures. Meanwhile, in curcumin have absorption on wave number of 3503.62 $cm^{-1}$for OH group, 1450–1630 cm^{-1} for groups C=O and C=C and 1024.69 cm^{-1}(COC). Fig. 4 show that FTIR spectrum of curcumin also appeared in the curcumin-SBA-15, although there is a little difference in intensity. This is likely due to the entrapment of curcumin in SBA-15 (15).

Differential scanning calorimetry (DSC) analysis

DSC analysis is one of thermal which can identify phase's change of a material like a temperature transition glass, melting temperature and heat flow as a function of temperature and time. Fig. 5 shows thermogram DSC of curcumin-SBA-15, SBA-15 and curcumin.

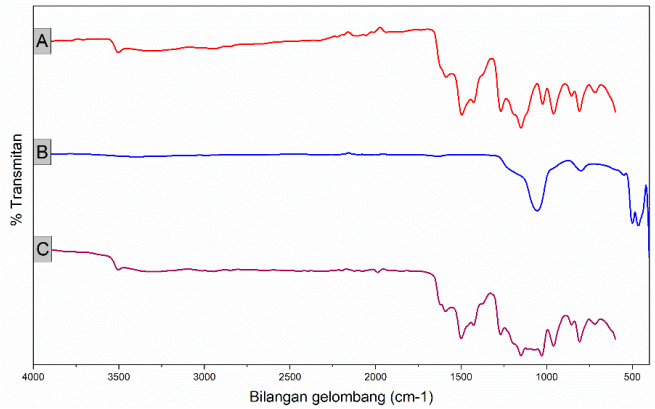

Fig. 4: FT-IR spectrum A) Curcumin, B) SBA-15, and C) Curcumin-SBA-15

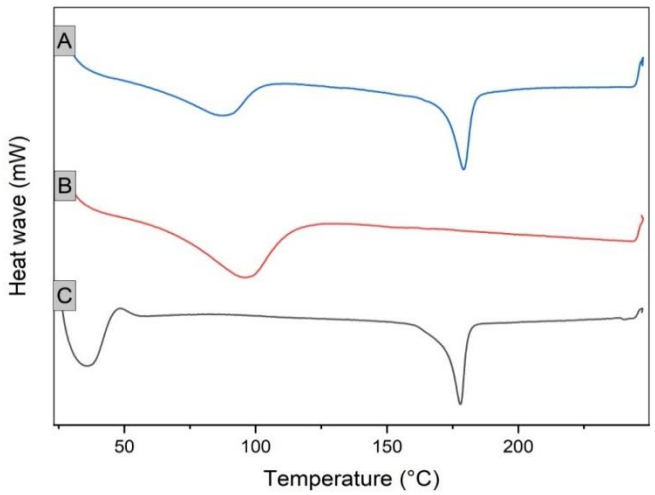

Fig. 5: DSC Thermogram A) Curcumin-SBA, B) SBA-15, and C) Curcumin

In the SBA-15 thermogram, it shows existence thermal glass transition at a temperature of 95.8 °C, which is only change the heat of capacity, not the phase of SBA-15. However, no melting peak of shown in DSC curve fig. 5. The absence of melting point phase transitions in the DSC analysis indicates that the samples are thermally stable at 250 °C. Thahir, 2019 who also did DSC analysis on SBA-15 yielded temperature transition glass at 74 °C and no peak for melting temperature [21].

The melting point of curcumin was 177 °C which shown by its sharp peak. However, the thermogram of curcumin-SBA-15 showed the glass transition of SBA-15 and the melting point of curcumin that indicated some curcumin was at the outside pore SBA-15 due to limitations of small pores size. According to BET analysis, almost whole surface SBA-15 pore adsorbed by curcumin is characterized with reduced pore volume in the curcumin-SBA-15 [22].

Scanning electron microscopy (SEM) analysis

Surface morphology of SBA-15, curcumin-SBA-15 and curcumin analyzed by SEM were presented in fig. 6. The results of SEM characterization on SBA-15 show rods grown together in fibers. This was also exhibited in previously research of SBA-15 synthesis. However, the morphology was no clear seen in the curcumin-SBA-15 sample because of the existence of curcumin in outside SBA-15 pores. SEM analysis only could observe morphology on the surface of the material but not for the internal structure of SBA-15 [23, 24].

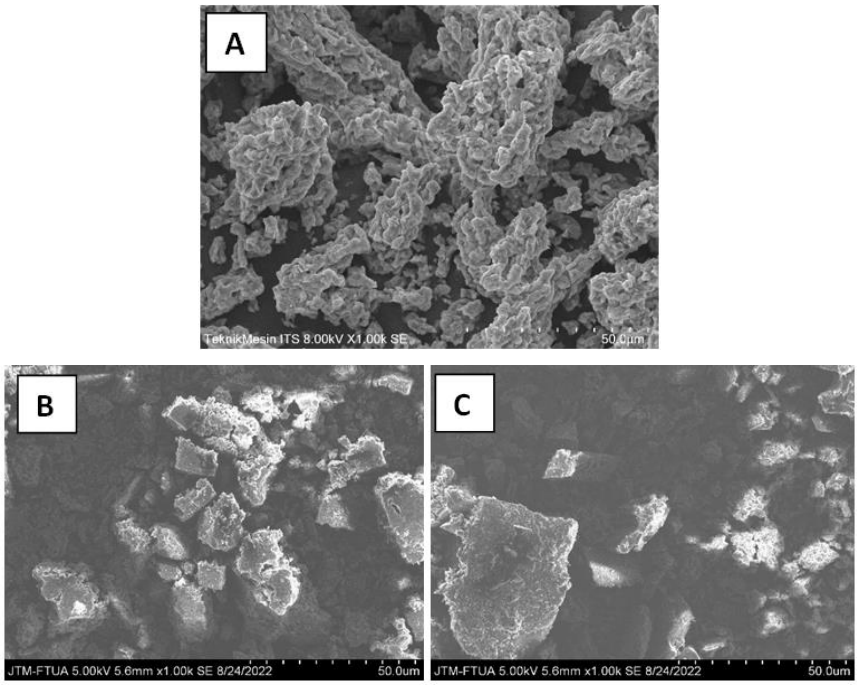

Fig. 6: Morphology on SEM A) SBA-15, B) Curcumin-SBA-15 and C) Curcumin

Solubility test

Table 3 depicts the enhancement solubility of curcumin-SBA-15 by 2.201 times compared to intact curcumin. Increasing solubility of curcumin due to reduce crystallinity of curcumin after adsorbed on the surface of SBA-15 which shown by the lower peak of PXRD intensity curcumin-SBA-15. Moreover, small pore sizes of curcumin-SBA-15 from results analysis nitrogen adsorption-desorption isotherm was 6 nm caused blockage growth crystal and increased surface area of curcumin-SBA-15 [12, 25]. Solubility test of curcumin and curcumin-SBA-15 was statistically tested and the result showed that solubility of each sample was significantly different ($p<0.05$).

Dissolution test

Table 4 shows that Curcumin-SBA-15 increased dissolution significantly ($p<0.05$) compared to intact curcumin. The average percentage dissolved of curcumin was 17.995±0.8965, while curcumin-SBA-15 was 57.827±0.5061 after 60 min. Fig. 7 shows the dissolution profile of curcumin in CO_2-free distilled water.

The improvement of dissolution in accordance to the PXRD of mesoporous that showed the lower intensity indicated the change from crystalline phase into amorphous. In addition, pore size analysis of Nitrogen Adsorption-Desorption Isotherm, showing that a significant decrease in pore volume of curcumin-SBA-15, indicated that almost the whole surface pore was adsorbed by curcumin. The small pore size of SBA-15 exhibit larger surface area contact between curcumin with the dissolution media, which performed improvement of curcumin and accordance with the Noyes-Whitney equation. Dissolution of curcumin-SBA-15 was also faster due to the bond formed among curcumin with silanol groups on the surface of SBA-15 are not too strong [26, 27].

Table 3: Solubility test results curcumin and curcumin-SBA-15

Sample	Average dissolution rate±SD (mg/100 ml)	Enhancement solubility
Curcumin	0.487±0.0084	-
Curcumin-SBA-15	1.073±0.0124	2.201 times

n = 3

Table 4: Dissolution result curcumin in CO2-free distilled water

Time (min)	% Average dissolution±SD	
	Curcumin	Curcumin-SBA-15
5	4.769±0.475	19.224±0.478
10	6.473±0.523	24.088±0.990
15	8.164±1.015	32.935±1.260
30	12.629±0.926	45.801±1.363
45	15.331±0.642	51.709±0.676
60	17.995±0.896	57.827±0.506

n = 3

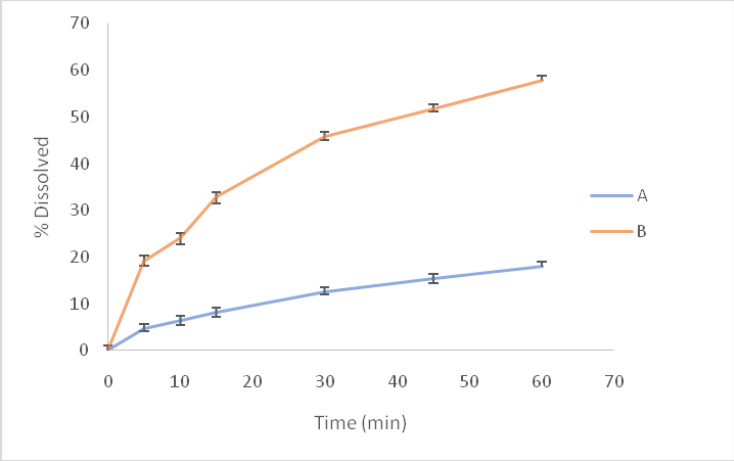

Fig. 7: Rate dissolution curcumin in CO_2-free distilled water, A) Curcumin and B) Curcumin-SBA-15

CONCLUSION

This study shows that that curcumin could adsorbed in mesoporous SBA-15, based on the results of thermal analysis characterization using DSC, X-ray diffraction pattern analysis, IR spectroscopic analysis, and morphological analysis with SEM. Curcumin-SBA-15 mesoporous SBA-15 is able to enhance the solubility and dissolution of curcumin, which was increased 2.201 times and 17.995% to 57.827%, respectively.

FUNDING

The authors would like to thank Universitas Andalas for granting this research under scheme Riset Dasar (No. T/7/UN16.17/PT.01.03/KO-RD/2021)

AUTHORS CONTRIBUTIONS

Conceptualization, LF, E. Z. and U. H.; methodology, L. F., U,H. and H,A., formal analysis, U. H., L. F., and H. A.; resources, E. Z., L,F., and U. H.,; writing-original draft preparation, L. F., and H. A.; writing-review and editing, L. F., H. A.,; supervision, E. Z; funding acquisition, E. Z. and L. F. All authors have read and agreed to the published version of the manuscript.

CONFLICT OF INTERESTS

The authors declare no conflict of interest.

REFERENCES

1. Liu Z, Smart JD, Pannala AS. Recent developments in formulation design for improving oral bioavailability of curcumin: a review. J Drug Deliv Sci Technol. 2020 Dec 1;60. doi: 10.1016/j.jddst.2020.102082.
2. Zheng B, McClements DJ. Formulation of more efficacious curcumin delivery systems using colloid science: enhanced solubility, stability, and bioavailability. Molecules. 2020 Jun 17;25(12):2791. doi: 10.3390/molecules25122791, PMID 32560351.
3. Zaini E, Fitriani L, Sari RY, Rosaini H, Horikawa A, Uekusa H. Multicomponent crystal of mefenamic acid and N-methyl-D-glucamine: crystal structures and dissolution study. J Pharm Sci. 2019 Jul 1;108(7):2341-8. doi: 10.1016/j.xphs.2019.02.003, PMID 30779887.
4. Gangurde AB, Kundaikar HS, Javeer SD, Jaiswar DR, Degani MS, Amin PD. Enhanced solubility and dissolution of curcumin by a hydrophilic polymer solid dispersion and its insilico molecular modeling studies. J Drug Deliv Sci Technol. 2015 Oct 1;29:226-37. doi: 10.1016/j.jddst.2015.08.005.
5. Kumar S, Malik MM, Purohit R. Synthesis methods of mesoporous silica materials. Mater Today Proc. 2017;4(2):350-7. doi: 10.1016/j.matpr.2017.01.032.
6. Ambrogi V, Perioli L, Marmottini F, Accorsi O, Pagano C, Ricci M. Role of mesoporous silicates on carbamazepine dissolution rate enhancement. Micropor Mesopor Mater. 2008 Aug 1;113(1-3):445-52. doi: 10.1016/j.micromeso.2007.12.003.
7. Abd-Elrahman AA, el Nabarawi MA, Hassan DH, Taha AA. Ketoprofen mesoporous silica nanoparticles SBA-15 hard gelatin capsules: preparation and *in vitro*/*in vivo* Characterization. Drug Deliv. 2016 Nov 21;23(9):3387-98. doi: 10.1080/10717544.2016.1186251, PMID 27167529.
8. Zhou Y, Quan G, Wu Q, Zhang X, Niu B, Wu B. Mesoporous silica nanoparticles for drug and gene delivery. Acta Pharm Sin B. 2018;8(2):165-77. doi: 10.1016/j.apsb.2018.01.007, PMID 29719777.
9. Laitinen R, Lobmann K, Strachan CJ, Grohganz H, Rades T. Emerging trends in the stabilization of amorphous drugs. Int J Pharm. 2013;453(1):65-79. doi: 10.1016/j.ijpharm.2012.04.066, PMID 22569230.
10. Yu C, Tian B, Fan J, Stucky GD, Zhao D. Salt effect in the synthesis of mesoporous Silica templated by non-ionic block copolymers. Chem Commun. 2001 Dec 21;(24):2726-7. doi: 10.1039/b107640j.
11. Nishi Y, Inagaki M. Gas adsorption/desorption isotherm for pore structure characterization. In: Materials science and engineering of carbon: characterization. Elsevier; 2016. p. 227-47.
12. Kakran M, Sahoo NG, Tan IL, Li L. Preparation of nanoparticles of poorly water-soluble antioxidant curcumin by antisolvent precipitation methods. J Nanopart Res. 2012 Mar 1;14(3). doi: 10.1007/s11051-012-0757-0.
13. Sulistyani M, Huda N. Perbandingan metode transmisi dan reflektansi pada pengukuran polistirena menggunakan instrumentasi spektroskopi fourier transform infrared. Indonesian J Chem Sci. 2018;7(2). Available from: http://journal.unnes.ac.id/sju/index.php/ijcs.
14. Cychosz KA, Thommes M. Progress in the physisorption characterization of nanoporous gas storage materials. Engineering. 2018;4(4):559-66. doi: 10.1016/j.eng.2018.06.001.
15. Jangra S, Girotra P, Chhokar V, Tomer VK, Sharma AK, Duhan S. *In vitro* drug release kinetics studies of mesoporous SBA-15-azathioprine composite. J Porous Mater. 2016 Jun 1;23(3):679-88. doi: 10.1007/s10934-016-0123-1.
16. Horikawa T, Do DD, Nicholson D. Capillary condensation of adsorbates in porous materials. Adv Colloid Interface Sci. 2011;169(1):40-58. doi: 10.1016/j.cis.2011.08.003, PMID 21937014.
17. Morishige K. Revisiting the nature of adsorption and desorption branches: temperature dependence of adsorption hysteresis in ordered mesoporous Silica. ACS Omega. 2021 Jun 22;6(24):15964-74. doi: 10.1021/acsomega.1c01643, PMID 34179641.
18. Alazzawi HF, Salih IK, Albayati TM. Drug delivery of amoxicillin molecule as a suggested treatment for covid-19 implementing functionalized mesoporous SBA-15 with aminopropyl groups. Drug Deliv. 2021;28(1):856-64. doi: 10.1080/10717544.2021.1914778, PMID 33928831.

19. Albayati TM, Salih IK, Alazzawi HF. Synthesis and characterization of a modified surface of SBA-15 mesoporous silica for a chloramphenicol drug delivery system. Heliyon. 2019 Oct 1;5(10):e02539. doi: 10.1016/j.heliyon.2019.e02539, PMID 31667391.
20. Shen SC, Ng WK, Chia L, Dong YC, Tan RBH. Stabilized the amorphous state of ibuprofen by co-spray drying with mesoporous SBA-15 to enhance dissolution properties. J Pharm Sci. 2010;99(4):1997-2007. doi: 10.1002/jps.21967, PMID 19816955.
21. Thahir R, W Wahab A, L Nafie N, Raya I. Synthesis of mesoporous Silica SBA-15 through surfactant set-up and hydrothermal process. Rasayan Journal of Chemistry. 2019 Jul 1;12(3):1117-26. doi: 10.31788/RJC.2019.1235306.
22. Budiman A, Aulifa DL. Encapsulation of drug into mesoporous silica by solvent evaporation: a comparative study of drug characterization in mesoporous silica with various molecular weights. Heliyon. 2021 Dec 1;7(12):e08627. doi: 10.1016/j.heliyon.2021.e08627, PMID 35005278.
23. Legnoverde MS, Simonetti S, Basaldella EI. Influence of pH on cephalexin adsorption onto SBA-15 mesoporous Silica: theoretical and experimental study. Appl Surf Sci. 2014 May 1;300:37-42. doi: 10.1016/j.apsusc.2014.01.198.
24. Udayakumar V, Pandurangan A. Synthesis of Hf/SBA-15 lewis acid catalyst for converting glycerol to value-added chemicals. Journal of Porous Materials. 2017 Aug 1;24(4):979-90. doi: 10.1007/s10934-016-0337-2.
25. De Azeredo HMC de. Production, solubility and antioxidant activity of curcumin nanosuspension. Vol. 42. Food Sci Technol Campinas. 2009;42:1240-53.
26. Zhang Y, Zhi Z, Jiang T, Zhang J, Wang Z, Wang S. Spherical mesoporous silica nanoparticles for loading and release of the poorly water-soluble drug telmisartan. Journal of Controlled Release. 2010 Aug;145(3):257-63. doi: 10.1016/j.jconrel.2010.04.029, PMID 20450945.
27. Hasanah U, Wikarsa S, Asyarie S. Various chloride salt addition in mesoporous material (SBA-15) synthesis and potential as carrier for dissolution enhancer. dvances in health sciences research. Atlantis Press. 2021;345-51. doi: 10.2991/ahsr.k.211105.050.